# Capping layer influence and isotropic in-plane upper critical field of the superconductivity at the $FeSe/SrTiO_3$ interface

Yanan Li,[1,2] Ziqiao Wang,[1] Run Xiao,[1] Qi Li,[1] Ke Wang,[3] Anthony Richardella,[1,3] Jian Wang,[2] and Nitin Samarth[1,*]

[1]*Department of Physics, The Pennsylvania State University, University Park, Pennsylvania 16802, USA*

[2]*International Center for Quantum Materials, School of Physics, Peking University, Beijing 100871, China*

[3]*Materials Research Institute, The Pennsylvania State University, University Park, Pennsylvania 16802, USA*

(Received 15 June 2020; revised 9 January 2021; accepted 12 February 2021; published 22 March 2021)

Understanding the superconductivity at the interface of $FeSe/SrTiO_3$ is a problem of great contemporary interest due to the significant increase in critical temperature ($T_c$) compared to that of bulk FeSe, as well as the possibility of an unconventional pairing mechanism and topological superconductivity. We report a study of the influence of a capping layer on superconductivity in thin films of FeSe grown on $SrTiO_3$ using molecular beam epitaxy. We used *in vacuo* four-probe electrical resistance measurements and *ex situ* magnetotransport measurements to examine the effect of three capping layers that provide distinct charge transfer into FeSe: insulating FeTe, nonmetallic Te, and metallic Zr. Our results show that FeTe provides an optimal cap that barely influences the inherent $T_c$ found in pristine $FeSe/SrTiO_3$, while the transfer of holes from a nonmetallic Te cap completely suppresses superconductivity and leads to insulating behavior. Finally, we used *ex situ* magnetoresistance measurements in FeTe capped FeSe films to extract the angular dependence of the in-plane upper critical magnetic field. Our observations reveal an almost isotropic in-plane upper critical field, providing insight into the symmetry and pairing mechanism of high-temperature superconductivity in FeSe.

DOI: 10.1103/PhysRevMaterials.5.034802

## I. INTRODUCTION

The study of superconductivity in single unit cell FeSe interfaced with $TiO_2$ terminated $SrTiO_3$ (STO) is motivated by the discovery of intriguingly high critical temperatures. While $T_c \sim 9.4$ K for bulk FeSe [1] and $T_c \sim 3.7$ K in two-layer FeSe films grown on bilayer graphene [2], *in situ* scanning tunneling spectroscopy (STS) measurements of single unit cell FeSe/STO and angle-resolved photoemission spectroscopy (ARPES) measurements show a gap closing critical temperature around 65 K [3–6]; one report of *in situ* transport measurements (still to be reproduced) even suggests that the $T_c$ might reach 100 K in this system [7]. This material system thus provides an exciting platform to investigate high $T_c$ superconductivity different from that in the more extensively studied cuprates. It has also been suggested to provide a pathway to achieve topological superconductivity [8–12].

To carry out *ex situ* transport measurements on these ultrathin FeSe films, a typical approach has used protective capping layers such as FeTe and amorphous Si. An onset $T_c$ is detected around 54.5 K for *ex situ* measurements [13], slightly lower than the value given by *in situ* STS measurements. To seek a better understanding of the role played by the protection layer, we conducted *in situ* and *ex situ* transport measurements on FeSe films grown on STO with various capping layers. By using *ex situ* Hall measurements, we studied the relationship between the charge transfer from the capping layer and its influence on the superconductivity in FeSe thin films. Our results indicate that an insulating capping layer (FeTe) and a metallic capping layer (Zr) have little influence on $T_c$. In strong contrast, when we use a Te capping layer, superconductivity is completely suppressed and a superconductor-to-insulator transition occurs at low temperature. This is likely due to the transfer of holes from the Te layer to interfacial FeSe.

We also used the FeSe/STO film with crystalline FeTe capping to study the angle-dependent in-plane upper critical field. This allowed us to study the pairing mechanism in FeSe. Previous experimental and theoretical investigations attribute the high $T_c$ gap to the cooperative effect of spin fluctuations, band-bending-induced charge transfer from STO, and interfacial electron-phonon interaction [14–18]. In addition, $s\pm$ wave superconductivity has been considered to be a likely candidate for the gap pairing symmetry in iron pnictide superconductors, where the pairing "glue" is mediated by spin fluctuations [19]. However, it is still debated whether an $s\pm$ wave can describe the superconductivity in FeSe/STO, where there is no hole band on the Fermi surface and the STO phonon mode likely participates in the pairing. In fact, various pairing symmetries have been proposed in this system, including plain *s* wave, $s{+}{+}$, $s\pm$ wave, and *d* wave [20–30]. Theoretical proposals and experimental investigations have yet to arrive at a unified conclusion about the pairing symmetry. As the angle dependence of the upper critical magnetic field ($H_{c2}$) can shed light on the gap symmetry, we carried out angle-dependent in-plane (*ab* plane) magnetoresistance measurements. Our observations support an almost isotropic in-plane $H_{c2}$ below $T_c$. We discuss this in relation to the proposed pairing symmetries

*Author to whom all correspondence should be addressed: nsamarth@psu.edu

 

and other effects that might mask an anisotropic gap, if one exists.

## II. EXPERIMENTAL METHODS

We grew FeSe films on $TiO_2$-terminated STO (001) substrates with atomically flat steps in a Scienta Omicron molecular beam epitaxy (MBE) system. The base pressure of our system is $10^{-11}$ torr. The Fe, Se, and Te were evaporated from thermal Knudsen effusion cells. Zr was evaporated using an electron beam evaporator at 7 kV and 100 mA. To obtain $TiO_2$-terminated STO substrates, we first pretreated commercial (Shinkosha, Japan) substrates by standard chemical etching with 90 °C deionized water (45 min) and 10% HCl solution (room temperature, 45 min). Then, we annealed the pretreated substrates in a tube furnace under oxygen flow at 980 °C for 3 h [13,15]. FeSe films with thickness between three and seven unit cells were then grown using the procedures described by Zhang *et al.* [13]. During the growth, the substrate was kept at 450 °C. The growth rate is around 0.15 layer/min. After growth, the sample was annealed at 500 °C for 2 h. Zr and Te capping layers were deposited at a substrate temperature $T_S = 20\,^{\circ}$C (as measured using a thermal imaging camera). The FeTe caps were deposited at $T_S = 350\,^{\circ}$C. The MBE system is connected *in vacuo* with a Scienta Omicron LT-Nano four-probe scanning tunneling microscope (STM) that allows four scanning tips to move independently on the sample surface. The *in situ* transport measurements were conducted in this system without exposing the films to air, and the distance between the tips is around 2 mm during the measurement. The *ex situ* transport measurements were conducted in a Quantum Design 9 T Physical Property Measurement System (PPMS), and the film samples are mechanically scratched into Hall bar devices for *ex situ* transport measurements.

Cross-sectional transmission electron microscope (TEM) specimens were prepared on an FEI Helios 660 focused ion beam (FIB) system. 1 kV final cleaning was applied after samples became electron transparent to avoid ion beam damage to the sample surfaces. The high angle annular dark field (HAADF) scanning transmission electron microscopy (STEM) was performed on an FEI STEM at 200 kV (Titan G2 60-300). Energy-dispersive x-ray spectroscopic (EDS) elemental maps were collected by using a SuperX EDS system (Bruker) under STEM mode.

## III. RESULTS AND DISCUSSION

### A. Capping layer influence

Figure 1(a) shows the temperature dependence of the four-probe resistance of an FeSe film before and after capping with various layers (FeTe, Zr, Te). The resistance is normalized to the value of 125 K. *In situ* measurements show that the zero-resistance $T_c$ of the bare FeSe film is around 26 K. After capping with FeTe, this *in situ* $T_c$ decreases slightly to 24 K. Earlier work has shown that postgrowth annealing at a relatively high temperature is an essential step for achieving high $T_c$ superconductivity in single unit cell FeSe/STO. It is speculated that this annealing removes excess Se and allows the transfer of electrons from STO into FeSe [31,32]. When we cap the pristine FeSe layer with FeTe, the Te flux is

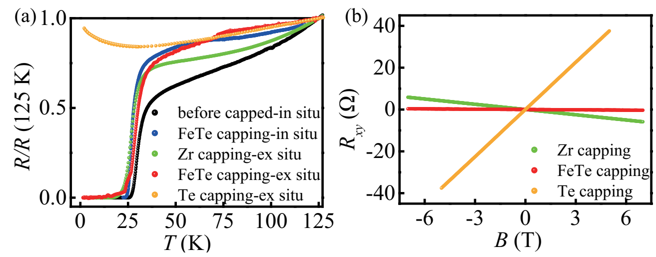


FIG. 1. Capping layer influence of superconductivity in FeSe films grown on STO. (a) Normalized temperature-dependent resistance of a FeSe film from *in situ* and *ex situ* electrical transport measurements. The FeTe capping layer decreases the $T_c$ of FeSe by around 2 K. All samples have FeSe thickness in the range of three to four unit cells. (b) *Ex situ* measurements of Hall resistance of an FeSe film with a Zr cap ($n = 6.9 \times 10^{18}$ m$^{-2}$), a FeTe cap ($n = 1.25 \times 10^{20}$ m$^{-2}$), and a Te cap ($p = 8.3 \times 10^{17}$ m$^{-2}$), respectively. It is measured at 50 K for FeTe capping and Zr capping, and at 30 K for Te capping. The FeTe capped sample has FeSe thickness of 7.5 UC. The other two samples have FeSe thickness in the range of three to four unit cells. The data are antisymmetrized in magnetic field.

usually 5–20 times larger than the Fe flux. The growth of FeTe introduces surplus Te onto the surface of FeSe/STO, introducing extra holes into the film, which might slightly suppress the $T_c$. Additionally, the growth of capping layers is likely to introduce impurities and defects into the film, which could also result in the decrease of the $T_c$. It should be noted that the decrease in $T_c$ caused by the overgrowth of FeTe is small (only ∼2 K).

From 125 K down to low temperature before the superconducting transition, the resistance of the film with a capping layer decreases more slowly than that of the film without a capping layer. All three types of capping layers decrease the residual resistivity ratio (RRR) of the FeSe film, indicating that all these capping layers likely introduce impurities and defects into the FeSe film. Figure 1(b) shows the Hall resistance of FeSe films capped with FeTe, Zr, and Te from *ex situ* transport measurements. Both the samples capped with FeTe and Zr show a superconducting transition at low temperature, and transport is dominated by *n*-type carriers (electrons). The FeSe film capped with only Te is not superconducting, but it displays an insulating transition at low temperature even though it shows metallic behavior at higher temperatures. Charge transfer from the Te capping layer changes the dominant carriers in the FeSe film from electrons into holes. This shows a capping layer induced insulator transition in FeSe film, similar to the insulator transition in as-grown *p*-type FeSe films or *p*-type FeSe films that have been annealed for a short time postgrowth [31,32].

Atomic resolution HAADF STEM measurements indicate that the Zr capping layer [Fig. 2(a)] is amorphous and that the crystallinity of the FeSe film is also slightly damaged by the capping process, although a superconducting transition is still observed by transport measurements. The circled area in the TEM image does not have as high crystalline quality as other areas. We note that the $T_c$ of the Zr capped FeSe samples is sensitive to the quality of the Zr capping layer. For example, $T_c$ is much lower in a Zr capped sample with

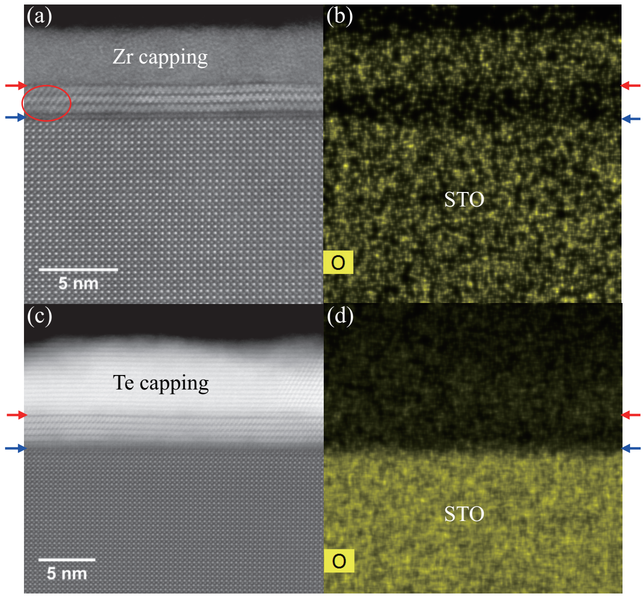


FIG. 2. Atomic resolution HAADF STEM images [(a) and (c)] and EDS mapping [(b) and (d)] of oxygen of FeSe film with Zr and Te. (a),(b) FeSe capped with Zr, (c),(d) FeSe capped with Te. The EDS results are on the same scale and the same region as the corresponding STEM images. The Zr layer has an amorphous structure and it partially destroys the crystalline structure of FeSe. The red-circled area does not have as high crystalline quality as other areas. The blue arrows indicate the interface between FeSe film and STO. The red arrows indicate the interface between FeSe film and the capping layer.

a disrupted crystalline structure as shown by TEM (Fig. S1 in the supplemental material [33]). It is likely that the high-energy Zr particles evaporated by the electron beam create damage when they impinge on the FeSe film. Growing the Zr capping layer at a much lower substrate temperature or lower e-beam power might be helpful to avoid this issue. Similar to FeTe capping, Te forms a crystalline capping layer as shown in Fig. 2(c). The electron dispersive spectroscopy (EDS) oxygen mapping results [Fig. 2(b)] show that Zr capping can capture oxygen and stop further oxidation of the FeSe film while Te protects the film by resisting the penetration of oxygen altogether [Fig. 2(d)]. We speculate that the oxidation of the thin Zr film is self-limiting, as found in single crystals of Zr [34]. However, compared with that earlier study [34], the oxidation depth of Zr might be different in our thin film samples due to the different deposition methods and storage conditions. EDS mapping of the elemental distribution in an FeSe film capped with Zr and Te (Figs. S2 and S3 in the supplemental material [33]) shows that the interface between Zr/Te and FeSe is clean: we do not detect Zr or Te signals in the FeSe film within the EDS resolution sensitivity limits. The interface between the FeSe film and crystalline FeTe/Te capping layers is cleaner than that between FeSe and a Zr capping layer.

Taking the transport results into consideration as well, this allows us to conclude that nonmetallic Te does not provide a good capping layer for protecting the thin FeSe film for *ex situ* experimental studies of its superconducting properties. Nonetheless, we note that an FeSe film capped with this kind of nonmetallic material can recover the superconducting transition after being decapped and annealed again at high temperature *in vacuo* [4]. Earlier studies have shown that electron doping on the surface of a monolayer FeSe film on STO by K cannot further increase the $T_c$ beyond the enhancement already obtained by interfacing with STO [35], which again suggests that the charge transfer and the phonon mode from STO work cooperatively to enhance the $T_c$ of this system. To further enhance the $T_c$ with a capping layer, some oxide capping layer that can transfer electron charge and contribute a phonon mode into the film is desirable. Our results demonstrate that the effect of the charge transfer from a capping layer can play an important role in the superconductivity of FeSe/STO. Understanding the influence of the capping layer is necessary in order to perform the *ex situ* measurements, especially if a consistent result between *in situ* and *ex situ* measurements is expected. Having gained some insight into the influence of the capping layer on superconductivity, we now discuss our attempts to understand the pairing symmetry in FeSe/STO. We use FeTe capping as the protective layer on top of FeSe for this purpose.

### B. Isotropic in-plane upper critical field

We carried out angle-dependent in-plane magnetoresistance measurements in FeTe/FeSe/STO samples both below and above $T_c$ to search for anisotropy of the magnetoresistance in the superconducting region. The presence or absence of an observed anisotropy can provide important insights into the pairing symmetry. We caution that such a measurement has to be carried out with great care since a very small misalignment ($<1^\circ$) between the plane of the sample and the magnetic field can easily result in a misleading artifact signal suggestive of an anisotropic magnetoresistance. Figure 3(a) shows the temperature dependence of the resistance, indicating the onset $T_c$ is around 45 K. Figure 3(a) shows the in-plane magnetoresistance at various temperatures. At first glance, we do indeed appear to observe an interesting anisotropy in the superconducting region, which weakens with increasing temperature and disappears gradually above $T_c$. However, by comparing the results from different mountings of the same sample, we have found that these oft-observed data are an example of the artifact mentioned above. For example, with a careful remounting of the sample accompanied by a rotation in the *ab* plane by 45°, the maximum and minimum angle of anisotropy of the magnetoresistance changed by a different value (not 45°) compared to the change of the sample orientation [see Fig. 3(c)]. The amplitude also changed. Similar measurements are reproduced in 10 distinct sample mountings and cool downs, but these measurements do not show a consistent anisotropy with in-plane critical field. As the sample was measured in the same instrument with the same setup for both orientations, these observations suggest that the anisotropy is more likely due to a small out-of-plane misalignment angle when mounting the sample rather than an intrinsic effect originating from the sample itself. To confirm this hypothesis, we plot the angle dependence of the critical field at 25 K extracted from the magnetic field dependence of the resistance (Fig. S4 in the supplemental material) [33] at various angles in Fig. 3(d). This anisotropic $H_{C2}$ can be fit

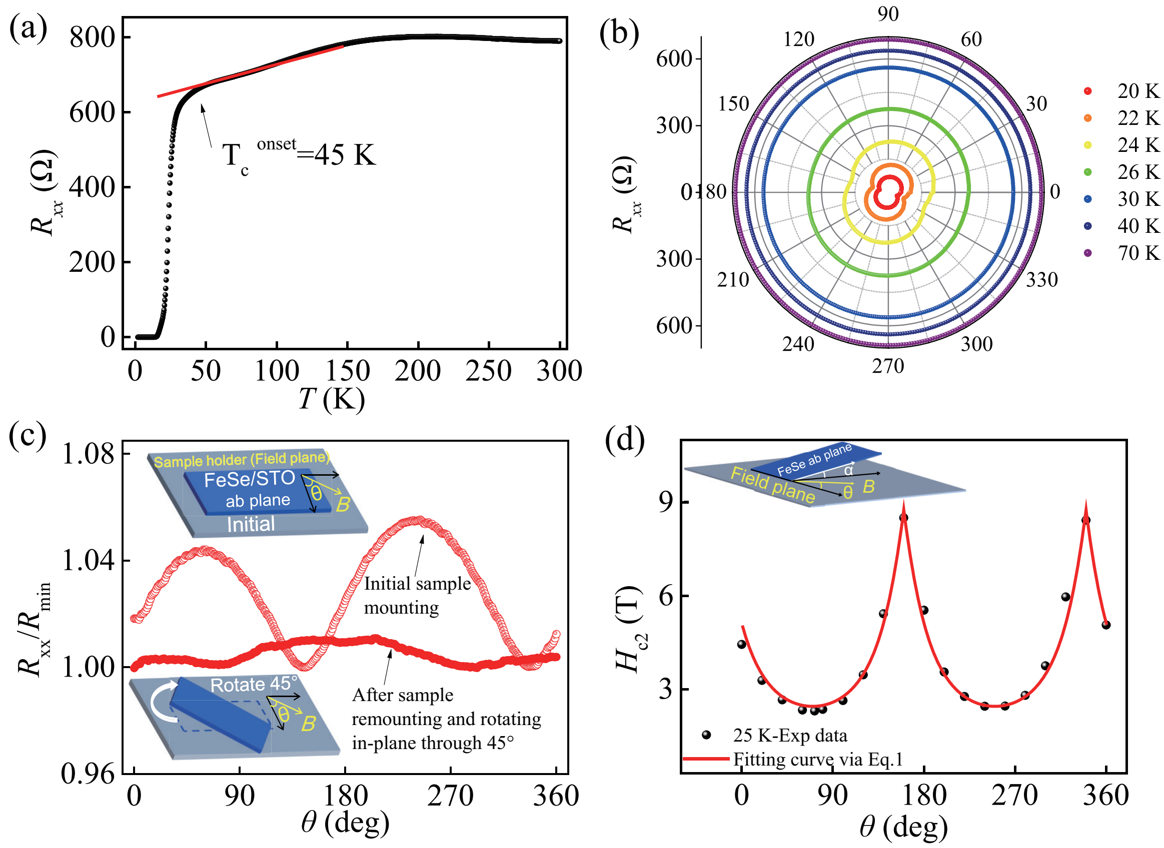


FIG. 3. Absence of anisotropy of the in-plane upper critical field of FeSe/STO. (a) Temperature-dependent resistance curve of an FeTe capped FeSe film, showing the superconductivity transition with onset $T_c$ around 45 K. The thickness of the film is estimated to be three unit cells. (b) Angle dependence of the in-plane magnetoresistance at various temperatures. (c) Comparison of the angle dependence of the magnetoresistance after rotating and remounting the sample in-plane through 45° taken at 18 K and 9 T. The angle position of the twofold symmetry shifts 70°, and the amplitude becomes smaller, which indicates that the twofold symmetry is not an intrinsic in-plane property of the FeSe film but rather arises from the out-of-plane misalignment. Insets are the schematics of the measurement setup. $\theta$ is the in-plane angle position, and $\alpha$ is the out-of-plane misalignment angle. The magnetoresistance is normalized to the minimum value of the magnetoresistance. (d) Angle dependence of the critical field extracted from resistance vs field curves at various angles at 25 K. The angle dependence (black dots are the experimental date) can be fit with the 2D Tinkham formula (red curve) by considering a fixed out-of-plane misalignment angle $\alpha$, confirming that the twofold symmetry is from the out-of-plane misalignment. Therefore, the in-plane critical field is isotropic within the resolution limit of the measurement.

with the 2D Tinkham formula [36]:

$$\left[\frac{H_{C2}(\theta')\sin(\theta')}{H_{C2}^{\parallel}}\right]^2 + \left|\frac{H_{C2}(\theta')\cos(\theta')}{H_{C2}^{\perp}}\right| = 1, \quad (1)$$

by considering a small misalignment angle $\alpha$ from the in-plane direction $\cos\theta' = \cos(\theta - 70^\circ)\sin(\alpha)$. [See the insets of Figs. 3(c) and 3(d) for definitions of the angles $\theta$ and $\alpha$.] Note that $\theta'$ is the effective angle between the magnetic field and the FeSe sample *ab* plane, and $\theta = 70^\circ$ (minimum of the upper critical field) is taken as the out-of-plane direction, while $\theta = 160^\circ$ (maximum of the upper critical field) is taken as the in-plane direction. GE varnish is used for mounting the sample, and a small misalignment angle between sample and sample holder is usually unavoidable. As the misalignment angle is random in both direction and amplitude when we mount the sample, the observed anisotropic magnetoresistance has a different peak position and oscillation amplitude. This "artificial" anisotropy is absent above $T_c$ because the magnetoresistance amplitude is very small above $T_c$. If we exclude the anisotropy due to the misalignment angle, our observations support an almost isotropic in-plane upper critical field (within the resolution limit of our instrument).

The upper critical field of a superconductor is determined by the interaction of an external applied magnetic field with the orbital and spin degrees of the charge in Cooper pairs via the orbital effect and Pauli paramagnetism [37]. When the orbital effect is considered, $H_{c2}$ is determined by the Fermi surface topology and the coupling parameter of the superconductor. Thus, the angular dependence of $H_{c2}$ can reveal insights into the pairing symmetry. For instance, *d*-wave superconductors usually show fourfold oscillations in the in-basal-plane angle-dependent $H_{c2}$ with the maximum along the antinodal direction and the minimum along the nodal direction [37]. ARPES measurements of interfacial FeSe/STO show that the Fermi surface is composed of two ellipsoidal electron pockets overlapping with each other at the Brillouin zone corner (four M-points) [38]. The superconducting gap is nodeless but moderately anisotropic with the gap maximum located along the major axis of the ellipse and the minimum along the intersection of two ellipsoidal electron pockets [38]. These observations could be consistent with a nodeless $d$-wave pairing scenario that is predicted when the relevant spin-orbit coupling energy of FeSe/STO is smaller than the superconducting gap [24]. We would then expect to observe an anisotropic in-plane dependence of the upper critical field in FeSe/STO; instead, we find that it is isotropic within the resolution limit of our measurements, suggesting the absence of an anisotropic superconducting gap. To reconcile our observations with the ARPES measurements, we consider three speculative but plausible explanations for observing an isotropic in-plane $H_{c2}$ below $T_c$. First, the isotropic in-plane magnetoresistance above $T_c$ [Fig. 3(b)] indicates that the scattering and spin orientation are isotropic. In this case, a weak anisotropy of the superconducting gap would be hidden by the isotropic scattering in the transport behavior. Second, the superconductivity in FeSe/STO might lie in the Bardeen-Cooper-Schrieffer (BCS) to Bose-Einstein condensation (BEC) crossover regime, near the unitary point [39]. In the BCS state, the fermions pair into bosonic Cooper pairs with a weak attractive interaction while the particles in the BEC state are all tightly bound bosonic pairs. In the BCS limit, fermions pair up and condense at the same critical temperature. In contrast, the particles in the BEC state first pair up and then condense below $T_c$. In this case, the evolution of critical parameters ($T_c$ and $H_{c2}$) would not reflect the gap symmetry when the superconductor is in the vicinity of the BEC state, and even an anisotropic superconducting gap would not result in an anisotropic critical field. Third, the orbital effect might be strongly suppressed when the superconductivity is quasi-two-dimensional (out-of-plane Fermi velocity is nearly zero). Consequently, the angle dependence of the in-plane $H_{c2}$ would be mainly determined by the angular dependence of the spin susceptibility and spin orbital coupling of the sample and thus would not reflect the gap symmetry.

## IV. CONCLUSIONS

To conclude, we studied the capping layer influence on superconductivity in FeSe/STO by combining *in situ* and *ex situ* electrical transport measurements. We found that an FeTe capping layer slightly decreases the $T_c$ of the FeSe film but otherwise preserves the superconducting properties for *ex situ* studies. Nonmetallic Te capping layers are not suitable for *ex situ* experimental study of FeSe/STO as they transfer holes into FeSe, inducing an insulator transition. E-beam evaporated Zr does protect the FeSe film from oxidization and preserves the superconductivity, but it also can damage the FeSe crystalline structure at the interface to some extent. Further explorations of alternate metallic capping layers are desirable. Finally, we used in-plane angle-dependent magnetoresistance measurements to demonstrate that the in-plane upper critical magnetic field of FeSe/STO is isotropic, contrary to expectations from prior ARPES measurements that indicate a moderately anisotropic superconducting gap. We proposed three possible scenarios that reconcile these observations.

## ACKNOWLEDGMENTS

This research was carried out using the Penn State Two-Dimensional Crystal Consortium-Materials Innovation Platform (2DCC-MIP) under NSF Grant No. DMR-1539916. We thank Cui-zu Chang and Timothy Pillsbury for their helpful suggestions in sample preparation. Y.L. acknowledges support from the University of Chicago. A.R. and N.S. acknowledge support from NSF Grant No. DMR-1539916. R.X. acknowledges support from the Institute for Quantum Matter under DOE EFRC Grant No. DE-SC0019331. Q.L. acknowledges support from DOE under Grant No. DE-FG02-08ER46531. J.W. acknowledges support from National Natural Science Foundation of China (No. 11888101).

[1] F.-C. Hsu, J.-Y. Luo, K.-W. Yeh, T.-K. Chen, T.-W. Huang, P. M. Wu, Y.-C. Lee, Y.-L. Huang, Y.-Y. Chu, D.-C. Yan, and M.-K. Wu, Superconductivity in the PbO-type structure $\alpha$-FeSe, Proc. Natl. Acad. Sci. (USA) **105**, 14262 (2008).

[2] C.-L. Song, Y.-L. Wang, Y.-P. Jiang, Z. Li, L. Wang, K. He, X. Chen, X.-C. Ma, and Q.-K. Xue, Molecular-beam epitaxy and robust superconductivity of stoichiometric FeSe crystalline films on bilayer graphene, Phys. Rev. B **84**, 020503(R) (2011).

[3] Q.-Y. Wang, Z. Li, W.-H. Zhang, Z.-C. Zhang, J.-S. Zhang, W. Li, H. Ding, Y.-B. Ou, P. Deng, K. Chang, J. Wen, C.-L. Song, K. He, J.-F. Jia, S.-H. Ji, Y.-Y. Wang, L.-L. Wang, X. Chen, X.-C. Ma, and Q.-K. Xue, Interface-induced high-temperature superconductivity in single unit-cell FeSe films on $SrTiO_3$, Chin. Phys. Lett. **29**, 037402 (2012).

[4] D. Liu, W. Zhang, D. Mou, J. He, Y.-B. Ou, Q.-Y. Wang, Z. Li, L. Wang, L. Zhao, S. He, Y. Peng, X. Liu, C. Chen, L. Yu, G. Liu, X. Dong, J. Zhang, C. Chen, Z. Xu, J. Hu, X. Chen, X. Ma, Q. Xue, and X. J. Zhou, Electronic origin of high-temperature superconductivity in single-layer FeSe superconductor, Nat. Commun. **3**, 931 (2012).

[5] S. He, J. He, W. Zhang, L. Zhao, D. Liu, X. Liu, D. Mou, Y.-B. Ou, Q.-Y. Wang, Z. Li, L. Wang, Y. Peng, Y. Liu, C. Chen, L. Yu, G. Liu, X. Dong, J. Zhang, C. Chen, Z. Xu, X. Chen, X. Ma, Q. Xue, and X. J. Zhou, Phase diagram and electronic indication of high-temperature superconductivity at 65 K in single-layer fese films, Nat. Mater. **12**, 605 (2013).

[6] R. Peng, H. C. Xu, S. Y. Tan, H. Y. Cao, M. Xia, X. P. Shen, Z. C. Huang, C. H. P. Wen, Q. Song, T. Zhang, B. P. Xie, X. G. Gong, and D. L. Feng, Tuning the band structure and superconductivity in single-layer FeSe by interface engineering, Nat. Commun. **5**, 5044 (2014).

[7] J.-F. Ge, Z.-L. Liu, C. Liu, C.-L. Gao, D. Qian, Q.-K. Xue, Y. Liu, and J.-F. Jia, Superconductivity above 100 K in single-layer FeSe films on doped $SrTiO_3$, Nat. Mater. **14**, 285 (2015).

[8] Z. F. Wang, H. Zhang, D. Liu, C. Liu, C. Tang, C. Song, Y. Zhong, J. Peng, F. Li, C. Nie, L. Wang, X. J. Zhou, X. Ma, Q. K. Xue, and F. Liu, Topological edge states in a high-temperature superconductor FeSe/$SrTiO_3$(001) film, Nat. Mater. **15**, 968 (2016).

[9] Z. Wang, C. Liu, Y. Liu, and J. Wang, High-temperature superconductivity in one-unit-cell FeSe films, J. Phys.: Condens. Matter. **29**, 153001 (2017).

[10] C. Liu, C. Chen, X. Liu, Z. Wang, Y. Liu, S. Ye, Z. Wang, J. Hu, and J. Wang, Zero-energy bound states in the high-temperature

superconductors at the two-dimensional limit, Sci. Adv. **6**, eaax7547 (2020).

[11] C. Chen, K. Jiang, Y. Zhang, C. Liu, Y. Liu, Z. Wang, and J. Wang, Atomic line defects and zero-energy end states in monolayer Fe(Te,Se) high-temperature superconductors, Nat. Phys. **16**, 536 (2020).

[12] C. Liu and J. Wang, Heterostructural one-unit-cell $FeSe/SrTiO_3$: From high-temperature superconductivity to topological states, 2D Mater. **7**, 022006 (2020).

[13] W.-H. Zhang, Y. Sun, J.-S. Zhang, F.-S. Li, M.-H. Guo, Y.-F. Zhao, H.-M. Zhang, J.-P. Peng, Y. Xing, H.-C. Wang, T. Fujita, A. Hirata, Z. Li, H. Ding, C.-J. Tang, M. Wang, Q.-Y. Wang, K. He, S.-H. Ji, X. Chen, J.-F. Wang, Z.-C. Xia, L. Li, Y.-Y. Wang, J. Wang, L.-L. Wang, M.-W. Chen, Q.-K. Xue, and X.-C. Ma, Direct observation of high-temperature superconductivity in one-unit-cell FeSe films, Chin. Phys. Lett. **31**, 017401 (2014).

[14] D.-H. Lee, Routes to high-temperature superconductivity: A lesson from $FeSe/SrTiO_3$, Annu. Rev. Condens. Matter Phys. **9**, 261 (2018).

[15] W. Zhao, M. Li, C.-Z. Chang, J. Jiang, L. Wu, C. Liu, J. S. Moodera, Y. Zhu, and M. H. W. Chan, Direct imaging of electron transfer and its influence on superconducting pairing at $FeSe/SrTiO_3$ interface, Sci. Adv. **4**, eaao2682 (2018).

[16] Q. Song, T. L. Yu, X. Lou, B. P. Xie, H. C. Xu, C. H. P. Wen, Q. Yao, S. Y. Zhang, X. T. Zhu, J. D. Guo, R. Peng, and D. L. Feng, Evidence of cooperative effect on the enhanced superconducting transition temperature at the $FeSe/SrTiO_3$ interface, Nat. Commun. **10**, 758 (2019).

[17] H. Zhang, D. Zhang, X. Lu, C. Liu, G. Zhou, X. Ma, L. Wang, P. Jiang, Q.-K. Xue, and X. Bao, Origin of charge transfer and enhanced electron–phonon coupling in single unit-cell FeSe films on $SrTiO_3$, Nat. Commun. **8**, 214 (2017).

[18] J. J. Lee, F. T. Schmitt, R. G. Moore, S. Johnston, Y. T. Cui, W. Li, M. Yi, Z. K. Liu, M. Hashimoto, Y. Zhang, D. H. Lu, T. P. Devereaux, D. H. Lee, and Z. X. Shen, Interfacial mode coupling as the origin of the enhancement of $T_c$ in FeSe films on $SrTiO_3$, Nature (London) **515**, 245 (2014).

[19] I. I. Mazin, D. J. Singh, M. D. Johannes, and M. H. Du, Unconventional Superconductivity with a Sign Reversal in the Order Parameter of $LaFeAsO_{1-x}F_x$, Phys. Rev. Lett. **101**, 057003 (2008).

[20] Q. Fan, W. H. Zhang, X. Liu, Y. J. Yan, M. Q. Ren, R. Peng, H. C. Xu, B. P. Xie, J. P. Hu, T. Zhang, and D. L. Feng, Plain s-wave superconductivity in single-layer FeSe on $SrTiO_3$ probed by scanning tunneling microscopy, Nat. Phys. **11**, 946 (2015).

[21] Z. Ge, C. Yan, H. Zhang, D. Agterberg, M. Weinert, and L. Li, Evidence for D-wave superconductivity in single layer $FeSe/SrTiO_3$ probed by quasiparticle scattering off step edges, Nano Lett. **19**, 2497 (2019).

[22] C. Chen, Q. Liu, W.-C. Bao, Y. Yan, Q.-H. Wang, T. Zhang, and D. Feng, Observation of Discrete Conventional Caroli–de Gennes–Matricon States in the Vortex Core of Single-Layer $FeSe/SrTiO_3$, Phys. Rev. Lett. **124**, 097001 (2020).

[23] C. Liu, Z. Wang, Y. Gao, X. Liu, Y. Liu, Q.-H. Wang, and J. Wang, Spectroscopic Imaging of Quasiparticle Bound States Induced by Strong Nonmagnetic Scatterings in One-Unit-Cell $FeSe/SrTiO_3$, Phys. Rev. Lett. **123**, 036801 (2019).

[24] D. F. Agterberg, T. Shishidou, J. O'Halloran, P. M. R. Brydon, and M. Weinert, Resilient Nodeless D-Wave Superconductivity in Monolayer FeSe, Phys. Rev. Lett. **119**, 267001 (2017).

[25] Y. Yamakawa and H. Kontani, Superconductivity without a hole pocket in electron-doped FeSe: Analysis beyond the Migdal-Eliashberg formalism, Phys. Rev. B **96**, 045130 (2017).

[26] J. Hu, Iron-Based Superconductors as Odd-Parity Superconductors, Phys. Rev. X **3**, 031004 (2013).

[27] X. Chen, S. Maiti, A. Linscheid, and P. J. Hirschfeld, Electron pairing in the presence of incipient bands in iron-based superconductors, Phys. Rev. B **92**, 224514 (2015).

[28] F. Yang, F. Wang, and D.-H. Lee, Fermiology, orbital order, orbital fluctuations, and cooper pairing in iron-based superconductors, Phys. Rev. B **88**, 100504(R) (2013).

[29] J. Kang and R. M. Fernandes, Superconductivity in FeSe Thin Films Driven by the Interplay Between Nematic Fluctuations and Spin-Orbit Coupling, Phys. Rev. Lett. **117**, 217003 (2016).

[30] C. Liu, Z. Wang, S. Ye, C. Chen, Y. Liu, Q. Wang, Q.-H. Wang, and J. Wang, Detection of bosonic mode as a signature of magnetic excitation in one-unit-cell FeSe on $SrTiO_3$, Nano Lett. **19**, 3464 (2019).

[31] Q. Wang, W. Zhang, W. Chen, Y. Xing, Y. Sun, Z. Wang, J.-W. Mei, Z. Wang, L. Wang, X.-C. Ma, F. Liu, Q.-K. Xue, and J. Wang, Spin fluctuation induced linear magnetoresistance in ultrathin superconducting FeSe films, 2D Mater. **4**, 034004 (2017).

[32] J. He, X. Liu, W. Zhang, L. Zhao, D. Liu, S. He, D. Mou, F. Li, C. Tang, Z. Li, L. Wang, Y. Peng, Y. Liu, C. Chen, L. Yu, G. Liu, X. Dong, J. Zhang, C. Chen, Z. Xu, X. Chen, X. Ma, Q. Xue, and X. J. Zhou, Electronic evidence of an insulator–superconductor crossover in single-layer $FeSe/SrTiO_3$ films, Proc. Natl. Acad. Sci. (USA) **111**, 18501 (2014).

[33] See Supplemental Material at http://link.aps.org/supplemental/10.1103/PhysRevMaterials.5.034802 for additional transport and TEM data.

[34] W. Ma, F. W. Herbert, S. D. Senanayake, and B. Yildiz, Non-equilibrium oxidation states of zirconium during early stages of metal oxidation, Appl. Phys. Lett. **106**, 101603 (2015).

[35] W. H. Zhang, X. Liu, C. H. P. Wen, R. Peng, S. Y. Tan, B. P. Xie, T. Zhang, and D. L. Feng, Effects of surface electron doping and substrate on the superconductivity of epitaxial FeSe films, Nano Lett. **16**, 1969 (2016).

[36] M. Tinkham, Effect of fluxoid quantization on transitions of superconducting films, Phys. Rev. **129**, 2413 (1963).

[37] J.-R. Wang, G.-Z. Liu, and C.-J. Zhang, Connection between in-plane upper critical field $H_{c2}$ and gap symmetry in layered d-wave superconductors, Phys. Rev. B **94**, 014501 (2016).

[38] Y. Zhang, J. J. Lee, R. G. Moore, W. Li, M. Yi, M. Hashimoto, D. H. Lu, T. P. Devereaux, D.-H. Lee, and Z.-X. Shen, Superconducting Gap Anisotropy in Monolayer FeSe Thin Film, Phys. Rev. Lett. **117**, 117001 (2016).

[39] S. Zhang, G. Miao, J. Guan, X. Xu, B. Liu, F. Yang, W. Wang, X. Zhu, and J. Guo, Superconductivity of the $FeSe/SrTiO_3$ interface in view of BCS-BEC crossover, Chin. Phys. Lett. **36**, 107404 (2019).